PHYSICAL REVIEW B **76**, 241201(R) (2007)

Effect of intramolecular disorder and intermolecular electronic interactions on the electronic structure of poly-*p*-phenylene vinylene

Ping Yang, Enrique R. Batista, Sergei Tretiak, Avadh Saxena, Richard L. Martin, and D. L. Smith*
Theoretical Division, Los Alamos National Laboratory, Los Alamos, New Mexico 87545, USA
(Received 26 November 2007; published 17 December 2007)

We investigate the role of intramolecular conformational disorder and intermolecular electronic interactions on the electronic structure of disorder clusters of poly-*p*-phenylene vinylene (PPV) oligomers. Classical molecular dynamics is used to determine probable molecular geometries, and first-principles density functional theory calculations are used to determine electronic structure. Intramolecular and intermolecular effects are disentangled by contrasting results for densely packed oligomer clusters with those for ensembles of isolated oligomers with the same intramolecular geometries. We find that in PPV electron trap states are induced primarily by intramolecular configuration disorder, while the hole trap states are generated primarily from intermolecular electronic interactions.

DOI: 10.1103/PhysRevB.76.241201 PACS number(s): 71.20.Rv, 71.55.Jv, 72.80.Le, 73.63.−b

The emergence of organic electronic devices, including light-emitting diodes and field-effect transistors, fabricated from conjugated polymers such as poly-*p*-phenylene vinylene (PPV),[1] has stimulated research into the electrical and optical properties of these semiconducting polymers. The nature of the charge trapping states, which stem from the conformational disorder in these systems, has not been clearly identified from a structural perspective. A complete description of these electronic materials is challenging because they are highly disordered and interactions between molecules are very important in determining their properties. Despite extensive experimental[2] and theoretical research,[3] there is still a limited understanding of these strongly interacting disordered materials. In this Rapid Communication, we use a combination of classical molecular dynamics (MD) and density functional theory (DFT) to investigate the electronic structure of densely packed clusters of PPV oligomers.

Statistically probable geometries of disordered clusters of PPV were simulated using classical MD. To isolate the effect of configurational disorder, we specifically consider clusters of five-ring PPV oligomers as studied experimentally in Ref. 4. Figure 1 shows the structure of one PPV oligomer [Fig. 1(A)], a crystal[4] of ordered oligomers [Fig. 1(B)], and an example of a disordered oligomer cluster from the MD simulations [Fig. 1(C)]. The unit cell used for the MD simulations and DFT calculations consisted of 12 five-ring oligomers, a total of 816 atoms.

Single crystals of PPV oligomers have been grown and structurally characterized.[4] Thin films of the polymer consist of small ordered regions, with a structure similar to that of the crystalline oligomers, separated by disordered regions.[5] The MD simulations are meant to describe the disordered regions. Substituted versions of PPV such as poly [2-methoxy, 5-(2′-ethyl-hexyloxy)-1,4-phenylene vinylene] (MEH-PPV) are frequently used in organic electronics. In these materials the substituted side groups, added primarily for processing reasons, are saturated and do not play a direct role in the electronic structure of the materials. However, in a condensed phase the substituted side groups tend to separate the conjugated segments of different molecules and thus reduce intermolecular electronic interactions compared to pristine conjugated polymers. Thus a combination of the crystal and an ensemble of disordered oligomer clusters serves as a model for the electronic structure of pristine PPV. And a combination of the isolated ordered oligomer and an ensemble of isolated disordered oligomers models the electronic structure of substituted PPVs.

A statistical sample of molecular geometries for the disordered PPV oligomers was generated by simulated annealing using periodic-boundary-condition MD with a modified MM3-2000 force field[6] as implemented in the TINKER code.[7] A new atom type was created to better reproduce the single and double C-C bond alternation and fitted to repoduce results from hybrid density functional calculations (B3LYP). The new force term was used in the linkage vinyl group, and the usual MM3-2000 force field was used for the remaining carbons. This combination of force field terms produced the difference between averaged length of all single bonds and double bonds of 0.19 Å. This is usually referred as the bond length alternation factor. In the simulated annealing calculations, the PPV oligomers were initially distributed randomly at extremely low density ($\rho \approx 0.01$ g/cm^3) and heated to 2000 K, and then pressure was applied to reach the experimental density of 1.25 g/cm^3. At this density the volume of

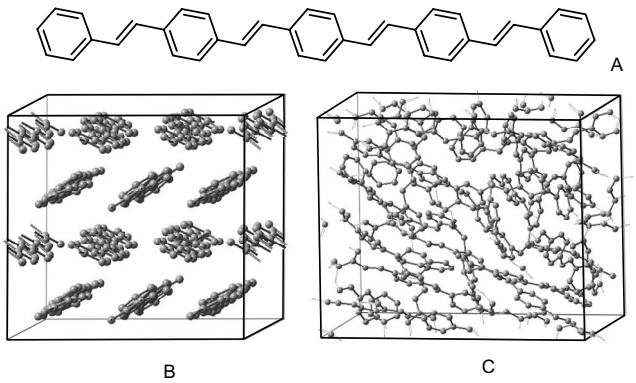

FIG. 1. (A) Molecular structure of the ordered oligomer. (B) Experimental crystal structure (Ref. 4). (C) Molecular structure of an oligomer cluster determined from the MD simulation. Hydrogen atoms are not shown for clarity.

the simulation cell was kept constant and the temperature cooled to 0 K.[8] Molecular geometries were extracted after the experimental density and 0 K were reached, and statistical samples were generated by repeating the simulated annealing procedure.

The electronic structure of the crystalline and disordered oligomer configurations were calculated using periodic-boundary-condition DFT at the generalized gradient approximation (GGA) level, using the PW91[9] functional.[8] The DFT calculations were performed at fixed geometries, determined from the MD simulations, using VASP,[10] with the projector-augmented-wave (PAW) scheme.[11] Due to the large size of the simulation cells (typically 20 Å on each side), Γ-point sampling of the Brillouin zone was adequate. This point was explicitly verified by adding an extra sampling k point in each direction. Use of the GGA leads to an underestimate of the energy gap, typical of pure DFT calculations. However, we are primarily interested in electronic states near the highest occupied and lowest unoccupied molecular orbital (HOMO and LUMO) energy levels separately and not in the absolute value of the energy gap.

The upper panel of Fig. 2 shows calculated energy levels for the ideal crystal and for 14 different disordered oligomer clusters, labeled $S1-S14$, whose geometries were determined from the MD simulations.[12] In order to make this comparison possible, the oligomers of the perfect crystal were optimized with our force field and overlapped at the experimental positions. The lower panel of Fig. 2 shows calculated energy levels for the ensemble of 12 isolated oligomers making up the clusters in the corresponding column of the upper panel. The lowest carbon 2s orbital of all the 14 configurations was found to have the same energy to within 0.01 eV. The effect of disorder on the electronic structure of the densely packed oligomer clusters can be separated into two components: intramolecular disorder and intermolecular electronic interactions. Intramolecular disorder is due to conformational deformations, resulting from the oligomers not being straight and planar, but kinked and twisted. These geometrical distortions interrupt the conjugation of the π orbitals, causing the electronic states to be more localized. Intermolecular interactions vary in the densely packed oligomer clusters because of differences in the local packing of the oligomers. The intermolecular π-π interactions depend strongly on the relative orientation of neighboring oligomers. To disentangle the effects of intramolecular conformational disorder and the intermolecular interaction effects on the energy level diagram, the electronic structure of each isolated oligomer in a cluster was computed independently (see lower panel of Fig. 2). The lack of repulsion among electron densities stabilizes the occupied levels, showing that the hole traps originate from the packing of the oligomers.

Panels (A)–(D) of Fig. 3 show calculated density of states for (A) the ideal crystal, (B) oligomer clusters $S4$ and (C) $S5$, and (D) the ensemble-averaged density of states for oligomer clusters $S1-S14$. Panels (E)–(H) of Fig. 3 show calculated density of states for (E) the undistorted oligomer in the ideal crystal, (F) the 12 isolated oligomers in clusters $S4$ and (G) $S5$, and (H) the ensemble-averaged density of states for the isolated oligomers in clusters $S1-S14$. The densities of states have been broadened using a Gaussian with full width at half maximum of 0.0272 eV.

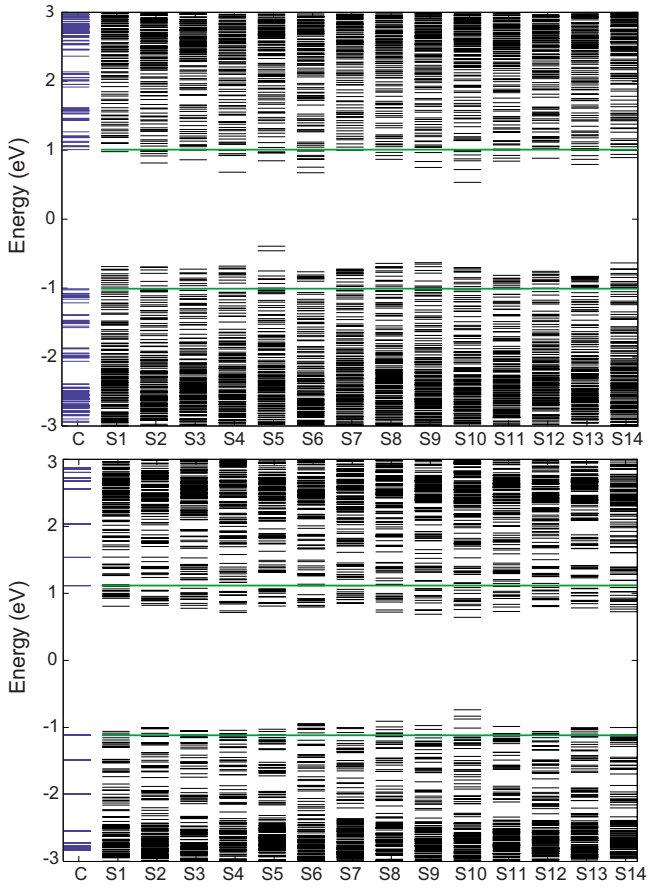

FIG. 2. (Color online) Energy level diagrams from the DFT calculations. The upper panel shows results for the ideal crystal (left) and 14 disordered oligomer clusters whose geometry was determined from the MD calculations; the lower panel shows results for an isolated ordered oligomer (left) and an ensemble of 12 isolated oligomers with the same molecular geometries as in the corresponding column of the upper panel.

The density of states for the isolated undistorted oligomer [see Fig. 3(E)] consists of a series of discrete states. In the crystal [see Fig. 3(A)] these discrete states are broadened into bands because of intermolecular electronic interactions. Because of these intermolecular interactions, the energy gap of the crystal is smaller than that of the isolated undistorted oligomer.[13] The packing pattern in the crystal is of the herringbone type, a common arrangement for conjugated oligomers without substitutions [Fig. 1(B)].[14] Intermolecular electronic interactions in crystals with the herringbone structure are relatively small due to the weak π-π overlap between oligomers. In the ensemble of distorted but isolated oligomers [Fig. 3(H)], the discrete lines of the undistorted oligomer are broadened by the statistical distribution of molecular distortions. Comparing Fig. 3(E) with Fig. 3(H) shows that this broadening in the valence states is nearly symmetric about the position of the corresponding valence state in the undistorted oligomer. In contrast, the distortions both broaden and shift to lower energy the conduction states compared to the corresponding conduction state in the undistorted oligomer. This can be traced to specific intramolecular interactions. The occurrence of *cis* configurations about the

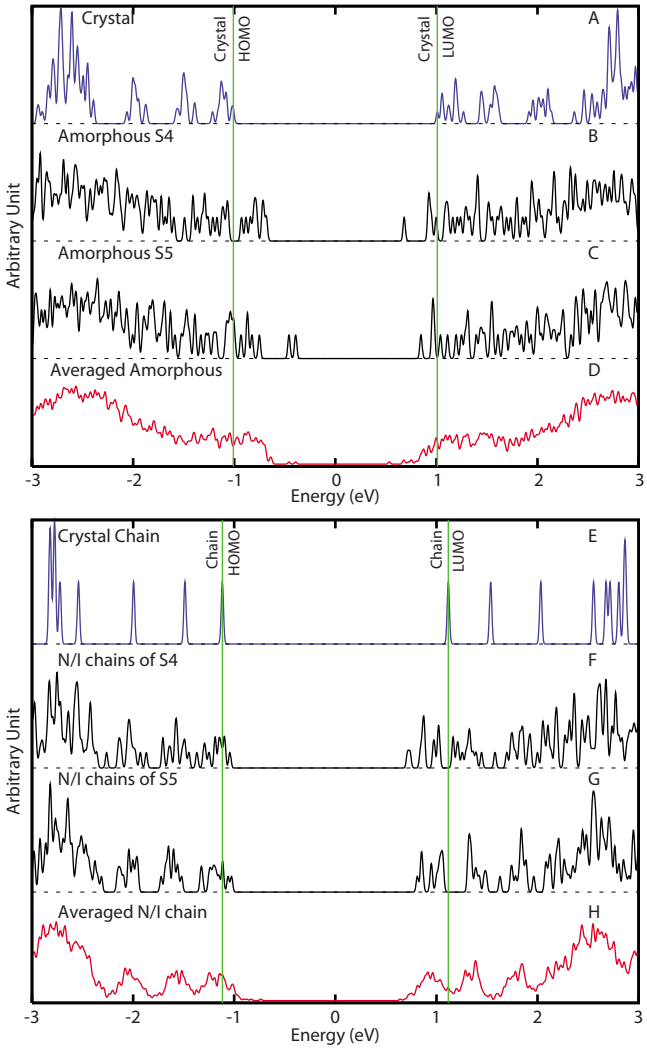

FIG. 3. (Color online) Calculated density of states for (A) the ideal crystal, (B) disordered cluster *S*4, (C) disordered cluster *S*5, (D) the ensemble average of clusters *S*1–*S*14, (E) the isolated oligomer in the ideal crystal, (F) the 12 isolated oligomers in cluster *S*4, (G) the 12 isolated oligomers in cluster *S*5, and (H) the ensemble average of isolated oligomers in clusters *S*1–*S*14. Note that the "vertical lines" denote different energy gaps in top panels (A)–(D) vs bottom panels (E)–(H).

vinylene linkages in some of the distorted oligomers tends to symmetrically reduce the HOMO-LUMO energy gap, whereas distortions of the bond lengths and angles in the vinylene linkages in some distorted oligomers tend to lower both the HOMO and LUMO energies. A combination of these two effects leads to the nearly symmetric broadening of the HOMO levels and the broadening and shift to lower energy of the unoccupied levels seen in Fig. 3(H). Contrasting Figs. 3(A) and 3(D), we see stronger intermolecular electronic interactions in the disordered oligomer clusters than in the crystal. This occurs because the π-π interactions are comparatively weak in the herringbone crystal structure where adjacent oligomer planes do not strongly overlap, but can be much larger in the disordered phase where adjacent oligomer planes can overlap strongly. Comparing the ensemble averaged results in Figs. 3(D) and 3(H) (and the corresponding single cluster cases [panel (B) with (F) and panel (C) with (G)]) shows that intermolecular interactions broaden and push both valence and conduction states to higher energy.

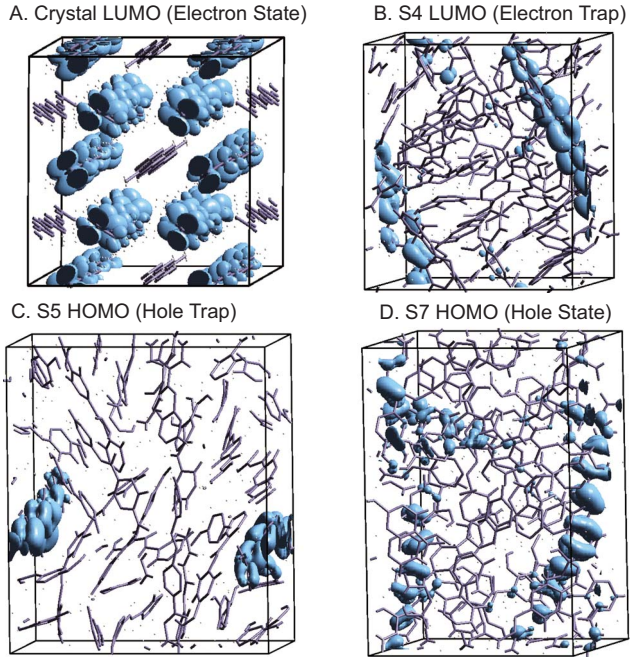

FIG. 4. (Color online) Calculated electron densities for selected states: (A) the crystal LUMO state, (B) the LUMO level for cluster *S*4, (C) the HOMO level for cluster *S*5, and (D) the HOMO level for cluster *S*7.

High-energy valence states can act as hole traps and low-energy conduction states can act as electron traps. As seen in Fig. 3, intramolecular distortions, on average, symmetrically broaden valence states and broaden and push conduction states to lower energy, whereas intermolecular electronic interactions, on average, broaden and push both valence and conduction states to higher energy. As a result, in PPV electron trap states are favored by intramolecular configurational disorder and hole trap states are favored by intermolecular electronic interactions. In substituted polymers, such as MEH-PPV, intermolecular electronic interactions are reduced compared to pristine polymers. Thus, hole traps should be more dominant in pristine PPV and electron traps more dominant in PPVs with long side chains.

Figure 4 shows the electron densities for selected one electron states. Figure 4(A) shows the electron density for the LUMO of the oligomer crystal. This state, like all the other states in the crystal, is delocalized throughout the crystal. By contrast, the HOMO and LUMO states in the disordered oligomer clusters are generally localized on individual molecules, whereas states further from the energy gap are often delocalized on more than one oligomer. Figure 4(B) shows the LUMO level for cluster *S*4. This state (see Fig. 2) is separated in energy from the other states in the cluster and lies deep within the energy gap of the corresponding crystal. It is strongly localized on a single oligomer. Figure 4(C) shows the HOMO level for cluster *S*5. This state is also separated in energy from the other states in the cluster, in the

energy gap of the corresponding crystal, and strongly localized. Figure 4(D) shows the HOMO level for cluster *S*7. This state is not strongly separated in energy from the other states in the cluster and not as deep into the energy gap of the corresponding crystal as the LUMO level on cluster *S*4 or the HOMO level on cluster *S*5. It is delocalized on several oligomers. The deep trap levels in the disordered clusters are usually localized on a single molecule. The *S*4 LUMO and *S*5 HOMO are examples of electron and hole trap, respectively, localized on one oligomer

By disentangling the effects from intramolecular versus intermolecular disorder, we found that in PPV electron trap states are induced primarily by intramolecular configurational disorder, while the hole trap states are generated primarily from intermolecular electronic interactions. Thin films of PPV consist of small ordered regions, with a local structure similar to that of the crystalline oligomers, separated by disordered regions. In substituted PPVs such as MEH-PPV the side groups separate the conjugated segments of different molecules and reduce intermolecular electronic interactions compared to pristine PPV. This effect was observed experimentally by Melzer *et al.*[15] whose experiment blended MDMO-PPV with PCBM (a substituted C_{60}) and found that the hole mobility increased by two orders of magnitude relative to neat MDMO-PPV. Our model suggests that hole traps should be more dominant in pristine PPV compared to PPV with long side chains due to the weak intermolecular electronic interactions in the latter. There are some experimental estimations for traps of up to 1.0 eV in depth[16] and polarization effects have been estimated at 0.1 eV.[17] Both these estimations are in good agreement with our calculations that predict traps of up to 0.6 eV. Because traps are important in determining electrical transport properties, these results provide strategies to design materials for good electrical transport.

In summary, we presented a computational methodology that combines classical molecular dynamics and density functional theory to study morphology effects in polymers. This approach was justified by applying it to one of the most studied organic polymers, PPV, to investigate the role of intramolecular conformational disorder and intermolecular electronic interactions on the electronic structure of disordered clusters.

This work was supported by DOE Office of Basic Energy Sciences under Work Proposal No. 08SCPE973. LANL is operated by Los Alamos National Security, LLC, for the NNSA of the U.S. Department of Energy under Contract No. DE-AC52-06NA25396.

*dsmith@lanl.gov

[1] J. H. Burroughes, D. Bradley, A. R. Brown, R. N. Marks, K. Mackay, R. H. Friend, P. Burns, and A. B. Holmes, Nature (London) **347**, 539 (1990).

[2] M. Wohlgenannt, X. M. Jiang, Z. V. Vardeny, and R. A. J. Janssen, Phys. Rev. Lett. **88**, 197401 (2002); F. Schindler, J. M. Lupton, J. Feldmann, and U. Scherf, Proc. Natl. Acad. Sci. U.S.A. **101**, 14695 (2004); C. Tanase, P. W. M. Blom, and D. M. de Leeuw, Phys. Rev. B **70**, 193202 (2004); C-Y Liu and S-A Chen, Macromol. Rapid Commun. **28**, 1743 (2007).

[3] V. Coropceanu, J. Cornil, D. A. da Silva Filho, Y. Olivier, R. Silbey, and J. Brédas, Chem. Rev. (Washington, D.C.) **107**, 926 (2007); E. Tutis, I. Batistic, and D. Berner, Phys. Rev. B **70**, 161202(R) (2004); J. G. S. Ramon and E. R. Bittner, J. Chem. Phys. **126**, 181101 (2007); L. Liu, D. Yaron, M. Sluch, and M. A. Berg, J. Phys. Chem. B **110**, 18844 (2006); P. Puschnig and C. Ambrosch-Draxl, Phys. Rev. B **60**, 7891 (1999); M. L. Tiago, J. E. Northrup, and S. G. Louie, *ibid.* **67**, 115212 (2003).

[4] P. F. V. Hutten, J. Wildeman, A. Meetsma, and G. Hadziioannou, J. Am. Chem. Soc. **121**, 5910 (1999).

[5] Y. B. Moon, S. D. D. V. Rughooputh, A. J. Heeger, A. O. Patil, and F. Wudl, Synth. Met. **29**, E79 (1989); C. Y. Yang, F. Hide, M. A. Díaz-García, A. J. Heeger, and Y. Cao, Polymer **39**, 2299 (1998).

[6] N. L. Allinger, Y. H. Yuh, and J.-H. Lii, J. Am. Chem. Soc. **111**, 8551 (1989); J.-H. Lii and N. L. Allinger, J. Phys. Org. Chem. **7**, 591 (1994); J. Comput. Chem. **19**, 1001 (1998).

[7] J. W. Ponder, TINKER: software tools for molecular design, version 3.8, Washington University School of Medicine, 2000.

[8] See EPAPS Document No. E-PRBMDO-76-R14748 for further computational details. For more information on EPAPS, see http://www.aip.org/pubservs/epaps.html.

[9] J. P. Perdew, in *Electronic Structure of Solids '91*, edited by P. Ziesche and H. Eschrig (Akademie Verlag, Berlin, 1991), p. 11; J. P. Perdew and Y. Wang, Phys. Rev. B **45**, 13244 (1992).

[10] G. Kresse and J. Hafner, Phys. Rev. B **47**, 558 (1993); **49**, 14251 (1994); G. Kresse and J. Furthmüller, Comput. Mater. Sci. **6**, 15 (1996); Phys. Rev. B **54**, 11169 (1996).

[11] G. Kresse and D. Joubert, Phys. Rev. B **59**, 1758 (1999); P. E. Blöchl, *ibid.* **50**, 17953 (1994).

[12] The energy levels shown in Fig. 2 correspond to the values obtained from the calculation and were neither shifted nor scaled before plotting them.

[13] P. Puschnig and C. Ambrosch-Draxl, Phys. Rev. B **60**, 7891 (1999); M. L. Tiago, J. E. Northrup, and S. G. Louie, *ibid.* **67**, 115212 (2003).

[14] D. C. Bott, C. S. Brown, J. N. Winter, and J. Barker, Polymer **28**, 601 (1987); S. Sasaki, T. Yamamoto, T. Kanbara, and A Morita, J. Polym. Sci., Part B: Polym. Phys. **30**, 293 (1992).

[15] C. Melzer, E. J. Koop, V. D. Mihailetchi, and P. W. M. Blom, Adv. Funct. Mater. **14**, 865 (2004).

[16] P. Stallinga, H. L. Gomes, H. Rost, A. B. Holmes, M. G. Harrison, and R. H. Friend, Synth. Met. **111-112**, 535 (2000); W. Graupner, G. Leditzky, G. Leising, and U. Scherf, Phys. Rev. B **54**, 7610 (1996).

[17] E. A. Silinsh, Phys. Status Solidi **3**, 817 (1970).